Magnetic Resonance Imaging 55 (2019) 1–6

Contents lists available at ScienceDirect

Magnetic Resonance Imaging

journal homepage: www.elsevier.com/locate/mri

Original contribution

Assessment of time-resolved renal diffusion parameters over the entire cardiac cycle

Rotem Shlomo Lanzman[1], Alexandra Ljimani*,[1], Anja Müller-Lutz, Julia Weller, Julia Stabinska, Gerald Antoch, Hans-Jörg Wittsack

University Dusseldorf, Medical Faculty, Department of Diagnostic and Interventional Radiology, D-40225 Dusseldorf, Germany

ARTICLE INFO

Keywords:
Diffusion magnetic resonance imaging
Renal circulation
Renal artery
Kidney
Magnetic resonance imaging

ABSTRACT

Object: To assess changes diffusion properties of renal cortex over the entire cardiac cycle using electrocardiogram-gated respiratory-triggered dynamic diffusion-weighted imaging (DWI).

Materials and methods: 20 healthy volunteers were investigated on a 1.5 T MR scanner. Blood flow velocity within the renal arteries was determined by electrocardiogram-gated phase-contrast measurements. For dynamic renal DWI, an electrocardiogram-gated respiratory-triggered coronal single-slice EPI sequence was acquired at 14 times at 20, 70, 120, 170, …, 570, 620, 720 ms after the R-wave over the cardiac cycle. ROI measurements were performed by two authors in the renal cortex on apparent diffusion coefficient (ADC) maps. A pulsatility index was calculated for ADC as maximal percentage change. Five subjects were measured twice to assess scan-rescan reproducibility.

Results: Flow measurements exhibited a minimum velocity of 15.7 ± 4.3 cm/s during the R-wave and a maximum of 43.2 ± 10.4 cm/s at 182.5 ± 48.3 ms after the R-wave. A minimal mean ADC of $2.19 \pm 0.09 \times 10^{-3}$ mm^2/s was observed during the R-wave. A maximum mean ADC of $2.85 \pm 0.20 \times 10^{-3}$ mm^2/s was measured 193 ± 57 ms after the R-wave. The mean ADC pulsatility index in the renal cortex was 29.9 ± 5.8%. ADC variation exhibited a significant correlation with pulsatile blood flow velocity. The scan-rescan reproducibility in this study had a low deviation of 0.3 ± 0.1%. The inter-reader reproducibility was 2.9 ± 0.6%.

Conclusion: Renal ADCs exhibit pulsatile characteristics. Due to the significant difference of systolic and diastolic ADCs, the pulsatility index can be calculated.

1. Introduction

Diffusion-weighted imaging (DWI) has emerged as a major functional MR imaging technique. DWI measures the motion of water molecules in the extracellular space, yielding the apparent diffusion coefficient (ADC) as a quantitative parameter. In the abdomen DWI is mainly used for the detection and characterization of tumors [1–4] or for functional evaluation of different organs [5–8]. Several studies have focused on renal DWI [7,9–14]. For both native and transplanted kidneys a significant correlation between diffusion parameters and renal function has been demonstrated [9,13,14]. Besides pure diffusion, renal ADC is also influenced by micro-perfusion and both contributions can be separated according to the IVIM (Intravoxel Incoherent Motion) model [15–17]. While the signal decay at b-values > 200 s/mm^2 is believed to reflect pure diffusion, at b-values ≤ 200 s/mm^2 it is mainly attributed to micro-perfusion. Recently, an ECG-gated temporally-resolved EPI sequence was introduced, which enables DWI measurements at different times of the cardiac cycle [18]. First results have shown that ADC values obtained at the time of maximum blood flow (systole) and minimum blood flow (diastole) differ significantly [18,19], highlighting the influence of perfusion on ADC values. So far, temporally-resolved DWI has only been acquired at two different times (systole and diastole) of the cardiac cycle. The purpose of this study was to obtain diffusion parameters over the entire cardiac cycle at multiple time points using

* Corresponding author at: University Dusseldorf, Medical Faculty, Department of Diagnostic and Interventional Radiology, Moorenstr. 5, D-40225 Dusseldorf, Germany.

E-mail addresses: Rotem.Lanzman@med.uni-duesseldorf.de (R.S. Lanzman), Alexandra.Ljimani@med.uni-duesseldorf.de (A. Ljimani), Anja.Lutz@med.uni-duesseldorf.de (A. Müller-Lutz), Julia.Stabinska@med.uni-duesseldorf.de (J. Stabinska), Antoch@med.uni-duesseldorf.de (G. Antoch), Wittsack@uni-duesseldorf.de (H.-J. Wittsack).

[1] Contributed equally, shared authorship.

https://doi.org/10.1016/j.mri.2018.09.009
Received 5 June 2018; Received in revised form 24 August 2018; Accepted 8 September 2018

dynamic DWI measurements with a temporal resolution of 50 ms.

2. Material and methods

Our study has been approved by the local ethics committee and has therefore been performed in accordance with the ethical standards laid down in the 1964 Declaration of Helsinki and its later amendments. All volunteers included in this study gave written informed consent prior to their inclusion in the study.

Twenty healthy subjects (10 men, 10 women, mean age = 26.2 ± 7.2 y) were included in this study and imaged on a 1.5 T whole-body clinical MRI scanner (Magnetom Avanto, Siemens Medical Systems, Erlangen, Germany) using a 6-channel array body coil and a 24-channel phased array spine coil integrated into the scanner table.

Coronal and axial T2-weighted single shot turbo spin echo (HASTE) were acquired (repetition time (TR) = 2000 ms, echo time (TE) = 79 ms, flip angle = 150°, 24 slices, thickness = 4 mm, field of view (FOV) = 380 mm, matrix = 320 × 260, parallel imaging factor = 2) for anatomical orientation.

For quantification of blood flow velocity in the renal arteries, ECG-gated phase-contrast flow imaging (gradient echo sequence, TE = 2.6 ms, TR = 71.6 ms, flip angle = 30°, matrix = 256 × 128, field of view = 320 mm, parallel imaging factor = 2, slice thickness = 6 mm, 20 phases within cardiac cycle) was performed in the parasagittal plane orthogonal to the renal arteries during breath-hold. Only one renal artery was measured per subject.

For dynamic DWI, an ECG-gated, respiratory-triggered echo-planar imaging (EPI) sequence was acquired in the coronal plane with 4 b values (0, 50, 100, 300 s/mm^2) using the following parameters: spin echo planar imaging sequence, TE = 66 ms, TR = 3000 ms, matrix = 192 × 192, FOV = 400 mm, 3 scan trace, 4 averages, 1 slice with 6 mm thickness, parallel imaging factor = 2. The acquisition was performed at 14 defined points at 20, 70, 120, 170, …, 570, 620, 720 ms after the R-wave of the ECG signal and data acquisition was only performed when the required respiratory state and the ECG-signal coincided. The acquisition time of a single image was about 100 ms and therefore short enough to enable temporally resolved measurements. Additionally, respiratory navigation assured that the images section of the kidneys was identically throughout the complete DWI scan, and no further image registration was needed. The total scan time ranged from 50 to 68 min (mean 58.6 ± 5.7 min) due to double triggering depending on the heart rate and respiration frequency. The quantitative analysis of the renal blood flow velocity was performed using Syngo Argus software (Syngo Argus, Siemens Medical Systems, Erlangen, Germany). Velocity time curves of the blood flow within the renal arteries were plotted.

Parametric images of the apparent diffusion coefficient (ADC) were calculated from the DWI data inline by the MRI scanner software as well as on an external workstation (Syngo MultiModality Workplace, Siemens Healthcare, Erlangen, Deutschland) using a mono-exponential model.

Image analysis was performed independently by two authors (A.L. 5 years of experience with abdominal MR imaging, R.S.L. 10 years of experience with abdominal MR imaging). To analyze ADC results in dependency of the underlying b-values, ADCs were calculated from sub-sets of images with b = 0, 50, 100 s/mm^2, b = 0, 300 s/mm^2, b = 0, 50, 300 s/mm^2, b = 0, 100, 300 s/mm^2 and b = 0, 300 s/mm^2 in three arbitrary subjects. Signal to noise ratio (SNR) of the ADC in renal cortex was determined as quality criteria with $SNR = \frac{\overline{ADC}}{\sigma_{ADC}}$, where $\overline{ADC}$ is the mean and σ_{ADC} is the standard deviation of a measured region. A comparison of the ADCs determined by sub-sets and full data was performed. This analysis was conducted with respect to reduce total measurement time for possible future investigations in patients.

Regional analysis of the ADC maps was conducted using home build software based on MATLAB (MathWorks, Natick, Massachusetts, USA). One continuous region of interest (ROI) (70–100 pixels) was drawn manually covering the whole cortical region (inter-reader variation < 10%). The mean value of the ROI was determined and plotted against the time within the cardiac cycle. Further an index of ADC pulsatility (PI_{ADC}) was calculated as

$$PI_{ADC} = \frac{ADC_{\max} - ADC_{\min}}{ADC_{\min}} \cdot 100\%,$$

where ADC_{max} and ADC_{min} are the maxima and minima of ADC values within the cardiac cycle. PI_{ADC} therefore reflects the maximal percentage change of ADC within the cardiac cycle. An analogous measure was defined for the blood flow velocity in the renal arteries:

$$PI_{flow} = \frac{F_{\max} - F_{\min}}{F_{\min}} \cdot 100\%,$$

where F_{max} and F_{min} are the global maximum and minimum blood flow velocities over the cardiac cycle.

The defined points in time within the cardiac cycle from the phase contrast flow measurement are depending on the individual heart cycle time using the pre-defined number of 20 measured phases. Therefore the points in time differed from the points in the DWI. For comparability of phase contrast flow measurements and dynamic diffusion parameters, the measured blood flow velocities were interpolated linearly to the pre-defined time points of DWI measurements using MATLAB R2011a (The MathWorks, Inc., Natick, Massachusetts, US).

In five subjects the MRI investigation was repeated to determine the reproducibility of measurements.

All calculated values are provided as mean and standard deviation. *t*-Test statistic was used to analyze differences between maximal and minimal ADC and blood flow velocity during the cardiac cycle. Further these differences were visualized in whisker plots. Pearson's correlation analysis was employed to compare ADC and blood flow velocity over the heart cycle. A p-value < 0.05 was defined as statistically significant.

3. Results

Dynamic DWI could be performed successfully in all 20 subjects. Cardiac cycle time varied between 754 ms und 1162 ms in our subjects.

Differences in the DWI signal decay and corresponding changes of ADC values in the renal cortex were observed at different times of the cardiac cycle (Figs. 1, 2).

Maximum ADC (ADC_{max}) determined numerically over all measurements in the renal cortex was 2.85 ± 0.20 × 10^{-3} mm^2/s at 193 ± 57 ms after the R-wave, while minimum ADC (ADC_{min}) found at 20 ms after R-wave was significantly lower at diastole (2.19 ± 0.09 × 10^{-3} mm^2/s) (p < 0.001). The mean of ADC over all points in time was ADC_{mean} = 2.43 ± 0.15 × 10^{-3} mm^2/s.

The maximum flow velocity within the renal arteries of 20 subjects was 43.2 ± 10.4 cm/s at 182.5 ± 48.3 ms after the R-wave, while the minimum flow velocity was significantly lower during diastole (15.7 ± 4.3) (p < 0.001).

Table 1 is containing the minimum and maximum data of ADC and blood flow velocity of all 20 subjects. The data are visualized in a boxplot in Fig. 3.

Mean pulsatility index (PI_{ADC}) measured over all subjects with 4 b-values was 29.9 ± 5.8% and mean pulsatility index of blood flow velocity in the renal artery (PI_{flow}) was 181.7 ± 51.8%.

Changes in ADC values in renal cortex exhibited a highly significant correlation with the pulsatile blood flow velocity in the renal arteries (r^2 = 0.95, p < 0.0001) (Figs. 4, 5).

3.1. b-Value optimization

The SNR differed between the ADCs resulting from sub-sets of images. Further the pulsatility index PI_{ADC} showed variations

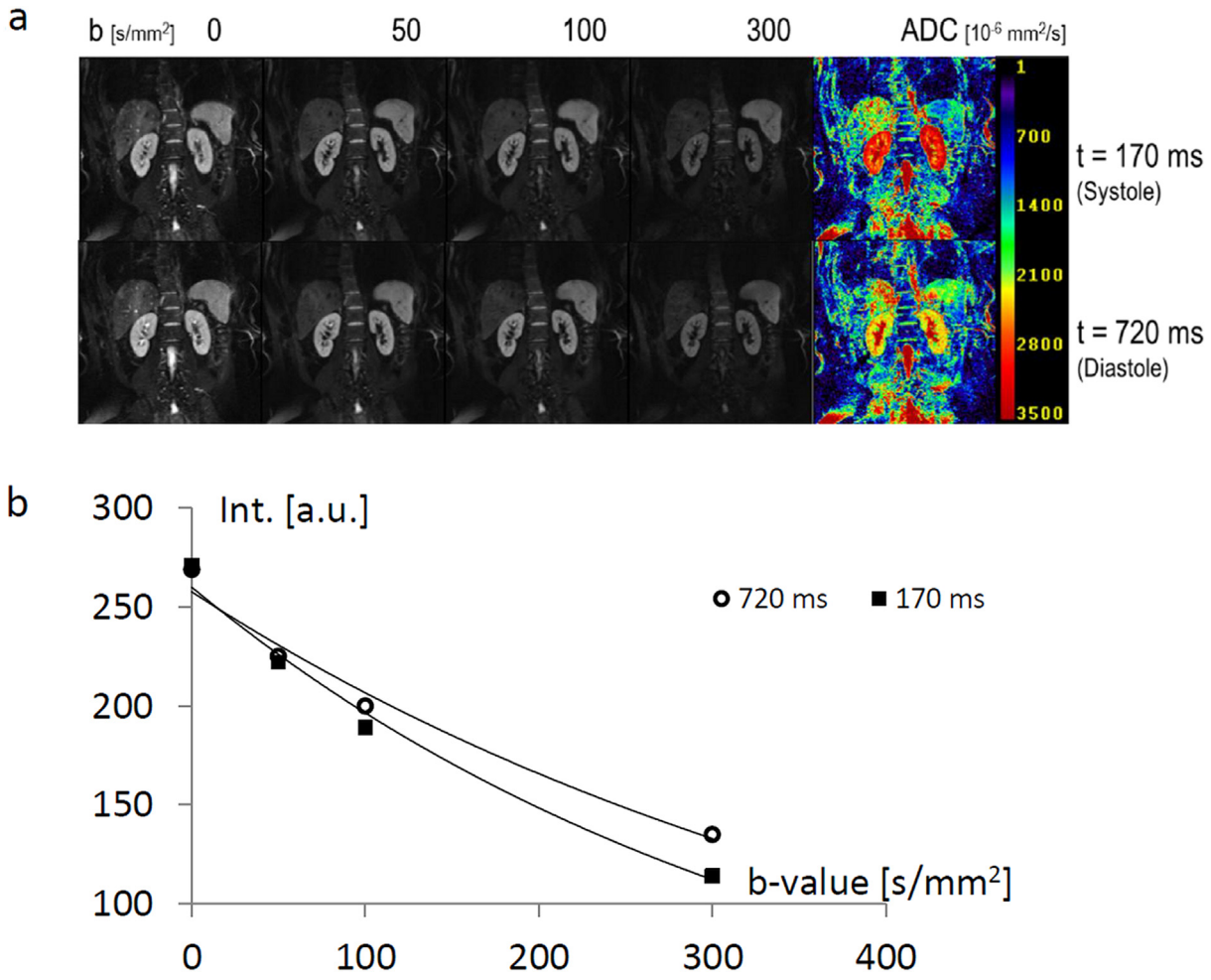

Fig. 1. Diffusion at 170 ms and 720 ms.
Fig. 1a shows diffusion-weighted images and corresponding ADC parameter maps of one representative subject acquired at systole and diastole. Fig. 1b demonstrates the corresponding diffusion depending MR signal decay in the renal cortex at systole and diastole.

depending on the different sub-sets (Table 1). The highest PI_{ADC} was calculated for the sub-set of b = 0, 50, 100 s/mm^2, but in this case SNR in the ADC maps was very poor due to the low difference between minimum and maximum b-values used. The highest SNR was obtained with the combination of b = 0, 300 s/mm^2. Although this subset resulted in a lower PI_{ADC}, the low standard deviation indicates that this subset might lead to stable results. With respect to potential savings in acquisition time, b = 0, 300 s/mm^2 might be a good compromise for future investigations (Table 2).

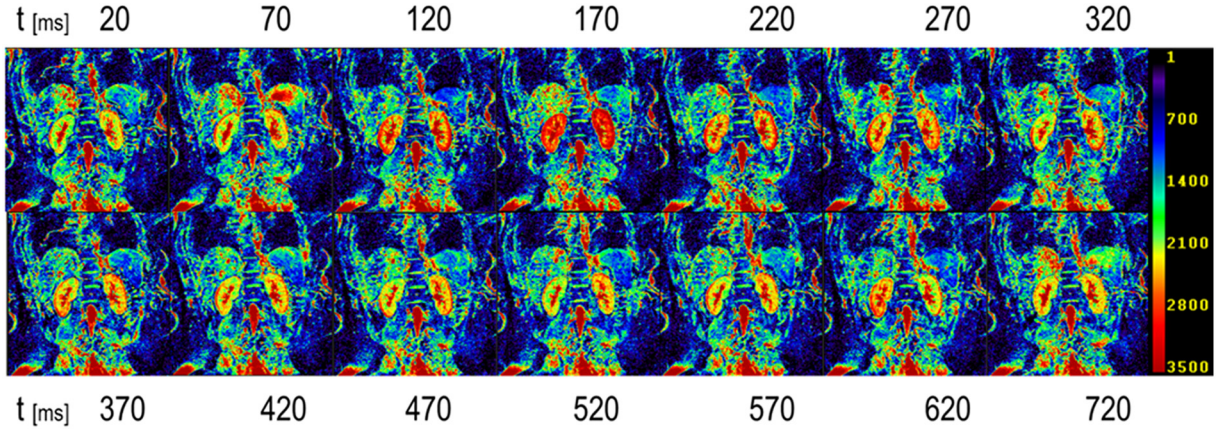

Fig. 2. ADC images at different times.
ADC parametric images of one representative subject acquired at 14 different times over the entire cardiac cycle; the maximum ADC signal at systole (170 ms after the R-wave) can be clearly appreciated.

Table 1
Minimum and maximum values of ADC and blood flow velocity for all subjects.

Subject	ADC_{max} [10^{-3} s/mm^2]	ADC_{min} [10^{-3} s/mm^2]	$Flow_{max}$ [cm/s]	$Flow_{min}$ [cm/s]
#1	2.87	2.07	50.5	15.2
#2	2.94	2.23	52.7	19.5
#3	2.75	2.25	31.0	12.6
#4	2.79	2.14	40.6	15.9
#5	2.85	2.25	44.4	16.6
#6	3.23	2.31	40.0	17.8
#7	2.52	2.07	26.3	8.2
#8	2.93	2.31	54.3	22.0
#9	2.76	2.12	21.6	11.5
#10	2.62	2.09	53.8	22.3
#11	2.70	2.10	33.4	10.4
#12	2.97	2.19	47.7	17.99
#13	2.81	2.27	37.6	9.1
#14	2.70	2.04	47.4	19.6
#15	2.73	2.17	39.4	10.9
#16	2.82	2.15	53.4	16.2
#17	3.41	2.38	54.1	20.6
#18	2.77	2.19	35.9	13.3
#19	2.88	2.29	57.4	19.4
#20	2.81	2.14	42.0	14.2
Mean ± sd	2.85 ± 0.20	2.19 ± 0.09	43.2 ± 10.4	15.7 ± 4.3

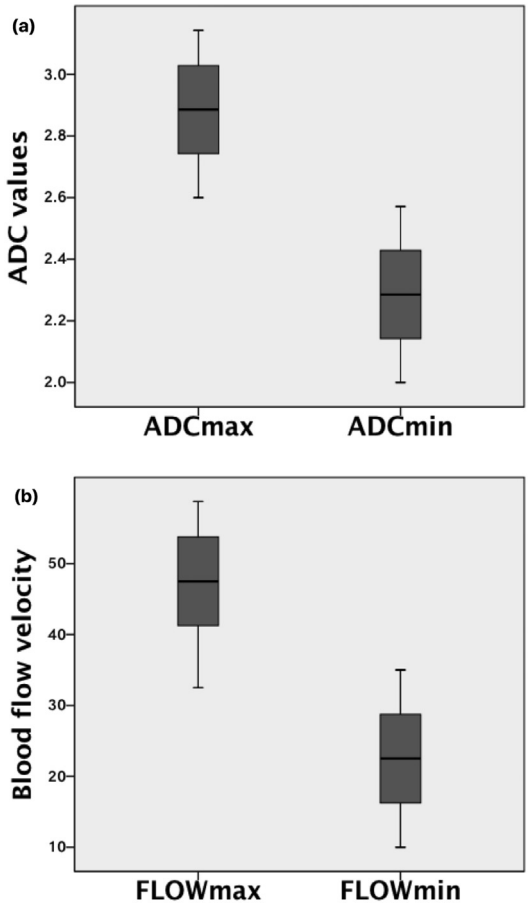

Fig. 3. Minimum and maximum ADC and blood flow velocity.
Box plots of minimum and maximum values of ADC [10^{-3} s/mm^2] (a) and blood flow velocity [cm/s] (b).

3.2. Reproducibility

In the five subjects that were scanned twice, PI_{ADC} exhibited a low deviation of 0.3 ± 0.1% between the first and second measurement. The inter-reader reproducibility of PI_{ADC} was 2.9 ± 0.6%.

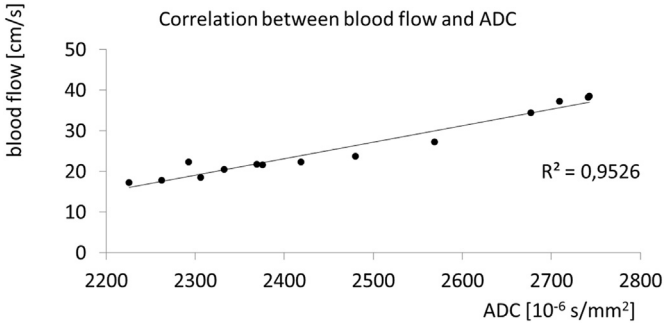

Fig. 4. Correlation between blood flow and ADC.
Correlation of mean ADC values in the renal cortex obtained at different times and the corresponding flow velocity measurements in the renal arteries of 20 subjects.

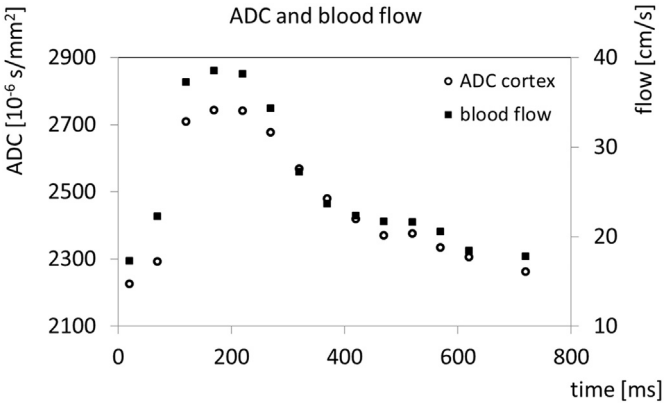

Fig. 5. ADC and blood flow versus time.
Mean ADC values in the renal cortex and mean blood flow velocity in the renal arteries of 20 subjects at different times of the cardiac cycle.

Table 2
Signal-to-noise-ratio (SNR) and PI_{ADC} as calculated with different b-value combinations.

b-Values [s/mm^2]	SNR in renal cortex	PI_{ADC}
0, 50, 100	5.86 ± 0.80	49.6 ± 17.9
0, 300	10.08 ± 0.85	26.3 ± 1.8
0, 50, 300	9.13 ± 0.22	31.7 ± 9.4
0, 100, 300	8.80 ± 0.15	32.3 ± 11.0
0, 50, 100, 300	9.24 ± 0.29	33.7 ± 10.9

4. Discussion

This is the first study to determine renal diffusion parameters at multiple points of the entire cardiac cycle. Our results demonstrate that ADC values vary significantly depending on the time of acquisition. These findings provide further evidence that ADC values are markedly influenced by perfusion. This influence is highlighted by the coincidence of the time of maximum ADC values in the renal cortex and maximum blood flow velocity in the renal artery around 180–190 ms following the R-wave. With low b-values, the DWI signal decay is mainly attributed to micro-perfusion [19]. Therefore, in our current study we used low b-values up to 300 s/mm^2 only. Consistently, with subsets of lower b-values (0, 50, 100 s/mm^2) we observed an increasing difference between systolic and diastolic ADC values as compared to subsets in which b = 300 s/mm^2 was included. However, SNR was significantly lower without b = 300 s/mm^2 than in subsets with b = 300 s/mm^2, indicating that results from these subsets with b-values 0–100 s/mm^2 might be more susceptible to variations.

The remarkable differences in ADC-values over the entire cardiac

cycle indicate that, beside the choice of b-values and differences in scanner geometry and field strength, pulsatile micro-perfusion might be a relevant factor for the variations in renal ADC values reported in the literature [7]. This assumption is supported by Binser et al., who have demonstrated that more reproducible ADC values can be obtained with a renal DWI protocol that contains cardiac-gating in addition to respiratory triggering [20].

Based on the differences in ADC parameters over the cardiac cycle we were able to calculate a pulsatility index for renal diffusivity (PI_{ADC}), which might serve as a novel biomarker. In both native and transplanted kidneys, the pulsatility index (PI) and the resistive index (RI) as obtained with Doppler ultrasound delivers valuable functional information [21–23]. For example, Doppler ultrasound studies have shown that renal PI might predict progression of chronic kidney disease in heart failure patients [21]. With Doppler ultrasound, PI or RI is measured in representative segmental or sub-segmental branches of the renal artery and changes in PI or RI are believed to reflect processes occurring in the renal parenchyma. However, Doppler ultrasound studies are known to have a high inter- and intraobserver variation [24]. The DWI technique presented in this study allows dynamic assessment of pulsatile changes of diffusion characteristics in the renal parenchyma itself and is more objective than ultrasound, as presented by a low scan-rescan and inter-reader variability. DWI has found increasing application in functional renal imaging. For example, several studies have highlighted the potential of DWI to monitor transplanted kidneys or to assess renal fibrosis [9,14,25,26]. Togao et al. have demonstrated a significant relationship between ADC values and histopathologic markers of fibrosis in an animal study, indicating that DWI might serve as a noninvasive biomarker for the assessment of renal fibrosis [26]. In renal fibrosis, the increase in cellular density restricts pure water diffusion in the extracellular space, which in turn leads to a decrease in ADC values. However, the decrease in ADC values is not specific for fibrosis. The herein presented approach might extend the spectrum of DWI for functional renal imaging, especially as pulsatile changes in renal ADC values, comparable to changes in Doppler RI and PI, might be influenced by renal stiffness. Further studies comparing ECG-gated dynamic DWI with MR elastography and MR perfusion measurements are required to understand and differentiate the contribution of blood flow and renal stiffness to PI_{ADC}.

The aim of the current study was to investigate the influence of blood pulsatility on renal ADC values over the entire cardiac cycle. As the cardiac output is strongly patient dependent, the biomarker PI_{ADC} would be erroneous determined by two arbitrary points only, as it was done in an earlier study by Wittsack et al. [18]. In this study we acquired DWI at 14 different points with 4 b-values and 4 signal averages, which resulted in a total acquisition time of approximately 60 min due to the double triggering approach. In view of the total acquisition time and in order to transfer dynamic DWI into clinical routine the acquisition time should be shortened dramatically. For this purpose, mono-exponential approach with few b-values should be preferred. Our results indicate, that acquisitions with two b-values (b = 0 and 300 s/mm^2) might be sufficient for calculation of PI_{ADC}. As SNR is high with b = 300 s/mm^2, the number of averages might be reduced from $n = 4$ to $n = 2$. These modifications in the imaging protocol could reduce scan time to about 15 min, which would make dynamic DWI adaptive for clinical research and imaging.

This study has several limitations. First limitation of our study is that only healthy volunteers were included. Hence, we cannot foretell whether PI_{ADC} has an additional diagnostic value in renal diseases. Therefore, studies including patients with diseases of native or transplanted kidneys are required. Besides for the minimization of the acquisition time only one renal artery per subject was measured. As all subjects were healthy volunteers, we supposed both renal arteries show the same blood flow. This might differ in healthy subjects having more than one renal artery on each side. However, none of our subjects demonstrate this anatomical peculiarity.

Second, as the herein presented technique consists of single-slice measurements, we were not able to cover the entire kidney. Coverage of the entire kidney might be crucial in case of focal pathologies, as for example in pyelonephritis. Development of a retrospective ECG-gating post-processing algorithm might be required in order to keep the acquisition time for multi-slice dynamic DWI constant. Further limitation of this study is the choice of the b-values. In this study only low b-values up to 300 s/mm^2 were acquired and the mono-exponential ADC quantification approach was used. Adding higher b-values up to 800–1000 s/mm^2 to the acquisition protocol might lead to more reliable ADC results with lower influence from pulsatility effects. Further changing the ADC quantification model from mono-exponential to IVIM might better reflect the influence of pulsatility on the fast component of the IVIM model. However, IVIM analysis requires a larger number of b-values for a reliable mathematical fitting with an overdetermined equation. Adding further b-values would result in longer acquisition times due to ECG- and respiratory triggering. Therefore, studies for the optimization of the acquisition protocol are needed.

5. Conclusions

In conclusion, we were able to demonstrate significant changes in renal ADC values over the entire cardiac cycle using an ECG-gated and respiratory triggered dynamic DWI technique. The excellent correlation between ADC parameters and renal blood flow at systole and diastole of the cardiac cycle highlights the influence of perfusion on ADC values. The novel ADC pulsatility index (PI_{ADC}) derived from pulsatile changes in ADC values might comprise additional information about renal tissue. Further patient studies are required to determine the clinical value of PI_{ADC} and to optimize the acquisition protocol for clinical application.

References

[1] Buchbender C, Hartung-Knemeyer V, Heusch P, Heusner TA, Beiderwellen K, Wittsack HJ, et al. Does positron emission tomography data acquisition impact simultaneous diffusion-weighted imaging in a whole-body PET/MRI system? Eur J Radiol 2013;82(2):380–4.
[2] Padhani AR, Liu G, Koh DM, Chenevert TL, Thoeny HC, Takahara T, et al. Diffusion-weighted magnetic resonance imaging as a cancer biomarker: consensus and recommendations. Neoplasia 2009;11(2):102–25.
[3] Sandrasegaran K, Sundaram CP, Ramaswamy R, Akisik FM, Rydberg MP, Lin C, et al. Usefulness of diffusion-weighted imaging in the evaluation of renal masses. AJR Am J Roentgenol 2010;194(2):438–45.
[4] Zhang J, Tehrani YM, Wang L, Ishill NM, Schwartz LH, Hricak H. Renal masses: characterization with diffusion-weighted MR imaging–a preliminary experience. Radiology 2008;247(2):458–64.
[5] Morani AC, Elsayes KM, Liu PS, Weadock WJ, Szklaruk J, Dillman JR, et al. Abdominal applications of diffusion-weighted magnetic resonance imaging: where do we stand. World J Radiol 2013;5(3):68–80.
[6] Thoeny HC, De Keyzer F. Extracranial applications of diffusion-weighted magnetic resonance imaging. Eur Radiol 2007;17(6):1385–93.
[7] Thoeny HC, De Keyzer F. Diffusion-weighted MR imaging of native and transplanted kidneys. Radiology 2011;259(1):25–38.
[8] Zhang JL, Morrell G, Rusinek H, Sigmund EE, Chandarana H, Lerman LO, et al. New magnetic resonance imaging methods in nephrology. Kidney Int 2014;85(4):768–78.
[9] Blondin D, Lanzman RS, Klasen J, Scherer A, Miese F, Kropil P, et al. Diffusion-attenuated MRI signal of renal allografts: comparison of two different statistical models. AJR Am J Roentgenol 2011;196(6):W701–5.
[10] Cheung JS, Fan SJ, Chow AM, Zhang J, Man K, Wu EX. Diffusion tensor imaging of renal ischemia reperfusion injury in an experimental model. NMR Biomed 2010;23(5):496–502.
[11] Muller MF, Prasad PV, Bimmler D, Kaiser A, Edelman RR. Functional imaging of the kidney by means of measurement of the apparent diffusion coefficient. Radiology 1994;193(3):711–5.
[12] Namimoto T, Yamashita Y, Mitsuzaki K, Nakayama Y, Tang Y, Takahashi M. Measurement of the apparent diffusion coefficient in diffuse renal disease by diffusion-weighted echo-planar MR imaging. J Magn Reson Imaging 1999;9(6):832–7.
[13] Xu Y, Wang X, Jiang X. Relationship between the renal apparent diffusion coefficient and glomerular filtration rate: preliminary experience. J Magn Reson Imaging 2007;26(3):678–81.
[14] Lanzman RS, Ljimani A, Pentang G, Zgoura P, Zenginli H, Kropil P, et al. Kidney transplant: functional assessment with diffusion-tensor MR imaging at 3T. Radiology 2013;266(1):218–25.

[15] Le Bihan D, Breton E, Lallemand D, Grenier P, Cabanis E, Laval-Jeantet M. MR imaging of intravoxel incoherent motions: application to diffusion and perfusion in neurologic disorders. Radiology 1986;161(2):401–7.
[16] Sigmund EE, Vivier PH, Sui D, Lamparello NA, Tantillo K, Mikheev A, et al. Intravoxel incoherent motion and diffusion-tensor imaging in renal tissue under hydration and furosemide flow challenges. Radiology 2012;263(3):758–69.
[17] Wittsack HJ, Lanzman RS, Mathys C, Janssen H, Modder U, Blondin D. Statistical evaluation of diffusion-weighted imaging of the human kidney. Magn Reson Med 2010;64(2):616–22.
[18] Wittsack HJ, Lanzman RS, Quentin M, Kuhlemann J, Klasen J, Pentang G, et al. Temporally resolved electrocardiogram-triggered diffusion-weighted imaging of the human kidney: correlation between intravoxel incoherent motion parameters and renal blood flow at different time points of the cardiac cycle. Invest Radiol 2012;47(4):226–30.
[19] Heusch P, Wittsack HJ, Heusner T, Buchbender C, Quang MN, Martirosian P, et al. Correlation of biexponential diffusion parameters with arterial spin-labeling perfusion MRI: results in transplanted kidneys. Invest Radiol 2013;48(3):140–4.
[20] Binser T, Thoeny HC, Eisenberger U, Stemmer A, Boesch C, Vermathen P. Comparison of physiological triggering schemes for diffusion-weighted magnetic resonance imaging in kidneys. J Magn Reson Imaging 2010;31(5):1144–50.
[21] Cicoira M, Conte L, Rossi A, Bonapace S, D'Agostini G, Dugo C, et al. Renal arterial pulsatility predicts progression of chronic kidney disease in chronic heart failure patients. Int J Cardiol 2013;167(6):3050–1.
[22] McArthur C, Geddes CC, Baxter GM. Early measurement of pulsatility and resistive indexes: correlation with long-term renal transplant function. Radiology 2011;259(1):278–85.
[23] Petersen LJ, Petersen JR, Ladefoged SD, Mehlsen J, Jensen HA. The pulsatility index and the resistive index in renal arteries in patients with hypertension and chronic renal failure. Nephrol Dial Transplant 1995;10(11):2060–4.
[24] Gottlieb RH, Snitzer EL, Hartley DF, Fultz PJ, Rubens DJ. Interobserver and intraobserver variation in determining intrarenal parameters by Doppler sonography. AJR Am J Roentgenol 1997;168(3):627–31.
[25] Eisenberger U, Thoeny HC, Binser T, Gugger M, Frey FJ, Boesch C, et al. Evaluation of renal allograft function early after transplantation with diffusion-weighted MR imaging. Eur Radiol 2010;20(6):1374–83.
[26] Togao O, Doi S, Kuro-O M, Masaki T, Yorioka N, Takahashi M. Assessment of renal fibrosis with diffusion-weighted MR imaging: study with murine model of unilateral ureteral obstruction. Radiology 2010;255(3):772–80.